

HIGH-RESOLUTION IMAGING OF TWO BIPOLAR PROTO-PLANETARY NEBULAE

SUN KWOK^{1,2}

Department of Physics and Astronomy, University of Calgary, Calgary, AB T2N 1N4, Canada

BRUCE J. HRIVNAK^{1,2}

Department of Physics and Astronomy, Valparaiso University, Valparaiso, IN 46383

AND

C. Y. ZHANG AND P. L. LANGILL

Department of Physics and Astronomy, University of Calgary, Calgary, AB T2N 1N4, Canada

Received 1996 April 8; accepted 1996 May 6

ABSTRACT

Sub-arcsecond resolution V and I images have been obtained for two proto-planetary nebulae. Both are found to show a definite bipolar morphology. A circumstellar disk is clearly seen in the $V-I$ color image, suggesting that the bipolar lobes are due to starlight scattered into the polar openings. This indicates that bipolar morphologies develop early in the evolution of planetary nebulae, even before the onset of photoionization.

Subject headings: circumstellar matter — planetary nebulae: general — stars: AGB and post-AGB

1. INTRODUCTION

One of the common properties of circumstellar matter in both the early and late stages of stellar evolution is the existence of “bipolar” morphologies. Young stars often show well-collimated outflows in opposite directions. The bipolar morphologies of planetary nebulae (PNs) have been noted for nearly a century (Curtis 1918), and modern high-quality optical and radio images have shown that a large fraction of PNs are not spherically symmetric (see Pottasch 1995). Microstructures made up of axisymmetric jetlike structures called FLIERS (fast, low-ionization emission regions; Balick et al. 1993) are now commonly found in PNs. The origin of the overall morphology of PNs and the detailed structures poses a major problem for our understanding of the dynamics of PNs. Since the nebulae of PNs originate from the remnants of the circumstellar envelopes, (CSEs) ejected by their progenitor asymptotic giant branch (AGB) stars, the fact that the CSEs of AGB stars are remarkably symmetric suggests that these morphologies are created or enhanced during the evolution from the AGB to the PN states.

In the past decade, there have been great advances in our understanding of the dynamical structure of PNs. It is believed now that the expansion and morphology of PNs are the result of the interaction between a fast radiatively driven central-star wind with the remnant CSE of the AGB progenitor (Kwok 1982; Balick 1987). Detailed hydrodynamical models confirm that many of the common morphologies of PNs can be produced by the interacting winds model (Frank & Mellema 1994; Mellema & Frank 1995).

While the dynamical models have been successful in explaining end results, they do not address the “cause” of the axial symmetry. Popular theories to create the density contrasts in the AGB CSE necessary for the formation of

axisymmetric nebulae include a binary companion and stellar rotation (Livo 1995). However, the question of “nurture” or “nature” remains: do the bipolar morphologies develop gradually as the interacting wind process progresses, as Balick (1987) suggests, or do they form early in the post-AGB evolution? A possible solution to this problem can be obtained by the observations of young PNs. If young PNs already show a similar morphological distribution as evolved PNs, then the bipolar nature is mainly inherited. On the other hand, if there exists a morphological sequence with age, then shaping by interacting winds is the dominant mechanism (Aaquist & Kwok 1996).

A more concrete test of this question is to observe the morphologies of proto-planetary nebulae (PPNs), objects in transition between the AGB and PN phases. This possibility is made even more tantalizing because the first two PPNs discovered, AFGL 618 and AFGL 2688, have bipolar morphologies (Westbrook et al. 1975; Ney et al. 1975). In recent years, an increasing number of PPNs have been discovered as the result of ground-based surveys of cool *IRAS* sources (see Kwok 1993). PPNs have the distinct characteristic of a “double peak” spectral energy distribution (SED), derived from the continuum radiation of both the central star (visible and near-infrared) and the remnant AGB CSE (mid-infrared). During our survey of cool *IRAS* sources, we found that although many PPN candidates have similar flux distributions in the infrared, their optical brightnesses differ greatly. From comparison with the known bipolar nebulae AFGL 618 and AFGL 2688, Hrivnak & Kwok (1991) interpreted these differences as the result of differing geometrical orientations of a circumstellar disk. The visibly bright objects have their disks orientated face-on, resulting in a double-peaked SED; the edge-on objects will be visually faint but have extended bipolar lobes (due to scattered light) in the plane of the sky.

However, due to the small angular extent of many of these PPN candidates, their morphologies are not obvious. In order to test this hypothesis, we have observed about 20 PPNs with a high-resolution camera on the Canada-France-Hawaii Telescope (CFHT). Two of them, IRAS 17441–2411 and IRAS 17150–3224, clearly show bipolar structures in visible light, while their SEDs exhibit double-

¹ Visiting astronomer at the Canada-France-Hawaii Telescope, operated by the National Research Council of Canada, the Centre National de Recherche Scientifique of France, and the University of Hawaii.

² Visiting astronomer at United Kingdom Infrared Telescope (UKIRT). UKIRT is operated by the Royal Observatories on behalf of the UK Particle Physics and Astronomy Research Council.

peaked behavior. The bipolar nature of IRAS 17150–3224 was discovered independently by Hu et al. (1993a). In this paper, we report on the photometric and high-resolution imaging observations of these two new bipolar PPNs.

2. OBSERVATIONS

2.1. Infrared Photometry

Mid-infrared and near-infrared observations of these two sources were obtained with the 3.8 m United Kingdom Infrared Telescope (UKIRT), using a Ge:Ga bolometer (UKT8) and an InSb photometer (UKT9). The initial location of the sources was made with the bolometer on 1989 August 16 (UT), as described below. Unfortunately, it was found later that there was a problem with the detector that limited the precision of the observations to about 20%; this was of sufficient accuracy to identify the sources, but not to make use of the photometry. IRAS 1744–2411 was reobserved with the bolometer on 1990 August 22, and photometry was obtained through the broadband N (10 μm) and Q (20 μm) and 30 μm filters using an aperture of 5".8 with an east-west chop of 20" at 12.5 Hz. The near-infrared observations were made on 1989 August 17, though the $JHKL'$ and narrower band M (nbM) filters. An aperture of 7".8 with a chop of 20" at 3.5 Hz was used.

In order to ensure that the correct optical counterparts of the *IRAS* sources were observed, we took particular care in the acquisition and identification of the targets. The telescope was moved first to the nearest bright SAO star of late spectral type and negligible proper motion. After peaking up on the signal of the star in the N filter, we marked the position of the source on the TV acquisition monitor. We then offset to the *IRAS* position and searched with the N filter until we found the location of the *IRAS* source and we peaked up on this. This assured that we had the correct position and object. In the case of IRAS 17441–2411, we went to the *IRAS* position and searched a box 30" \times 30" without finding the infrared source at 10 μm . We then began to move the telescope toward the nearby infrared source AFGL 5385, which is located 65" east. The *IRAS* source was located after moving about 40" east. We have determined the coordinates of this object to be R.A. = 17^h44^m09^s.7 and decl. = –24°11'47" (1950.0). We assume that the *IRAS* and AFGL sources are the same object. Our N and Q observations (see below) are in good agreement with those found for AFGL 5385 (Price & Murdock 1983); their positional difference is presumably due to the large aperture (10') used in the AFGL survey in what is a crowded field near the galactic center ($l = 4.2, b = 2.2$).

The observed magnitudes and details of the filters are listed in Table 1. Additional near-infrared observations of IRAS 17150–3224 were obtained by P. Whitelock using

the 1.9 m telescope of the South African Astronomical Observatory (SAAO) on 1988 March 31, and kindly made available to us. These are also listed in Table 1, and are in very close agreement with our measurements. These measurements for IRAS 17150–3224 are also in good agreement with the $JHKLM$ measurements of van der Veen, Habing, & Geballe (1989) and very close agreement with those of Hu et al. (1993a), except for the L and M magnitudes of Hu et al., which are much (1 mag) bright. It is not clear whether this discrepancy is the result of observational error or some real variability in the source, although the latter seems unlikely. For IRAS 17441–2411, one must be careful in comparing observations with those in the literature, since the source is located far from the *IRAS* position, and in this location near the galactic center there are many possible near-infrared sources with which to confuse it. From the descriptions of their observations and the listed coordinates, it seems that Hu et al. (1993b), observing also in the mid-infrared, have identified correctly the *IRAS* source, while van der Veen et al., observing the near-infrared and visible, have not. Whitelock (p. 1996, private communication) also attempted to observe this object, and she obtained values similar to ours. However, she presumably did not know the correct position, and thus it is doubtful that she actually observed the same object. We have not included these observations here. Our observations agree reasonably well with those of Hu et al., except for their M observation, which is much (0.8 mag) brighter.

2.2. Optical Imaging and Photometry

High-resolution CCD images were obtained with the 3.6 m CFHT on the nights of 1990 August 27 (nonphotometric) and 1991 June 4 and 6 (photometric). The DAO/CFHT image-stabilizing High-Resolution Camera (HRCam) was used in the fast guide mode. Details of the design of the HRCam are given by McClure et al. (1989). An SAIC 1080 \times 1080 pixel CCD detector was used with HRCam. Mounted on the CFHT prime focus, each pixel projects an angular size of 0".13 on the sky. Broadband V and I (Mould) and narrow-band $H\alpha$ ($\Delta\lambda = \sim 100$ Å) filters were used in the observations. Seeing conditions during the observations were very good; the stellar image sizes (FWHM) in the best images averaged 0".7, and their values are given in Table 2.

The images were calibrated using standard procedures, including bias subtraction and flat-fielding. Since the sky was rotated during the exposures, the calibrated images were first flipped and then rotated based on the rotation angle of the bonnette mirror recorded in the image headers. It was found that an additive constant of 12.5 had to be added to the nominal bonnette angle in order to recover the correct orientation, that is, north at the top and east to the left. Care was taken to make sure that the V and I images

TABLE 1
OBSERVED MAGNITUDES

<i>IRAS</i> Name	J	H	K	L	L'	nbM	N	Q	30 μm	Observatory
	$\lambda(\Delta\lambda)$ in μm									
$\lambda(\Delta\lambda)(\mu\text{m})$	1.23(0.28)	1.64(0.29)	2.18(0.42)	3.45	3.80(0.70)	4.76(0.62)	10.5(3.0)	19.5(5.2)	30	
17150–3224	11.02(2)	10.24(2)	9.51(2)	...	8.06(2)	6.78(6)	UKIRT
	11.00 ^a	10.19 ^a	9.49 ^a	8.46(5)	SAAO
17441–2411	11.33(2)	10.33(2)	9.61(2)	...	7.74(2)	6.54(3)	0.30(3)	–2.44(4)	–3.4(3)	UKIRT

^a Uncertainty $< \pm 0.05$ mag.

TABLE 2
RESULTS OF OBSERVATIONS

IRAS NAME	INTEGRATION TIME (s)			RESOLUTION (FWHM) (arcsec)			MAGNITUDE		
	<i>V</i>	H α	<i>I_c</i>	<i>V</i>	H α	<i>I_c</i>	<i>V</i>	<i>I_c</i>	COLOR
17150–3224	1200	600	300	0.72	0.75	0.88	14.48 \pm 0.02	12.52 \pm 0.03	1.96 \pm 0.02
17441–2411	900	...	150	0.71	...	0.66	15.58 \pm 0.02	13.04 \pm 0.03	2.54 \pm 0.03

were registered with each other to better than a few tenths of a pixel. The *V* and *I* images of IRAS 17150–3224 and 17441–2411 are displayed in Figures 1 and 2, respectively, along with the plate scale.

The images of IRAS 17150–3224 show that it is clearly

extended and elongated, with an angular size of 15".9 \times 8".7 in *V*, 15".2 \times 8".4 in *I*, and 14".7 \times 8".1 in H α (not plotted). The position angle is similar in all three images, $\sim 125^\circ \pm 2^\circ$, as measured from the line connecting the two peaks. There is also an obvious change in morphology with

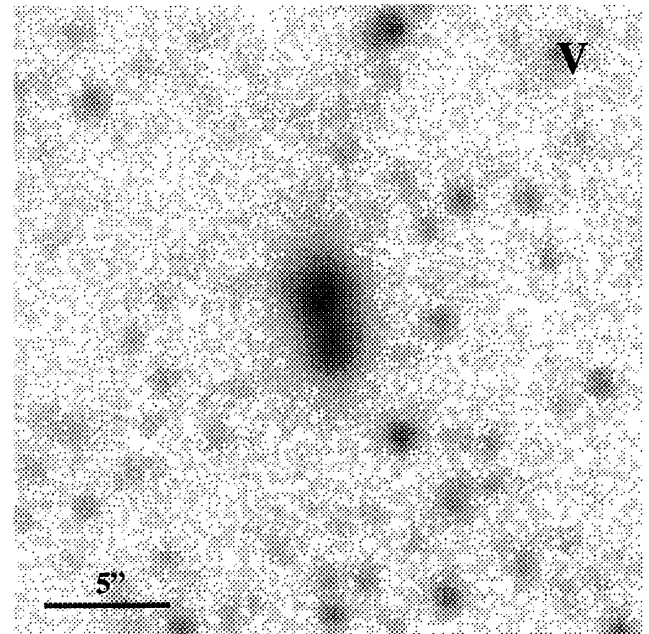
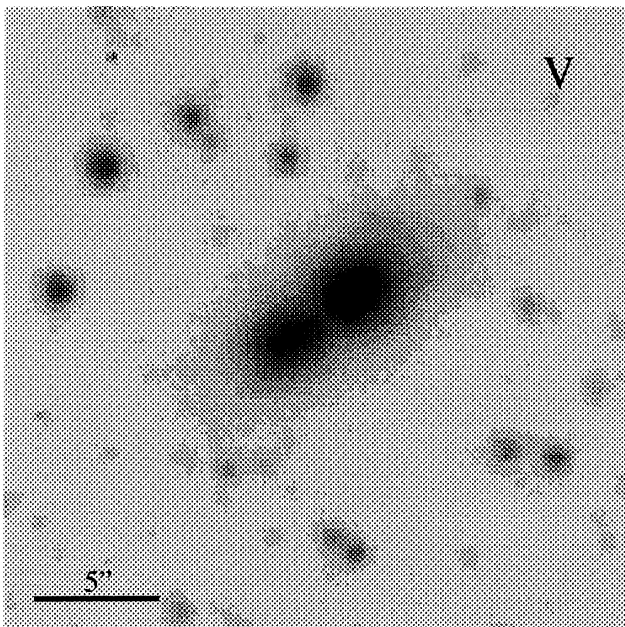


FIG. 1.—The gray-scale high-resolution *V* and *I* images of IRAS 17150–3224. North is to the top, east is to the left.

FIG. 2.—The gray-scale high-resolution *V*- and *I*-band images of IRAS 17441–2411.

wavelength. The V image displays two distinctly separate brightness peaks, with a separation of $3''.0$. The $H\alpha$ image is similar with a separation of $2''.8$. In the I image, the north-west peak has shifted to the southeast by $\sim 0''.25$ (with respect to the field stars), approximately along the line connecting the two peaks in the V image. The southeast peak is no longer distinct, but instead a ridge of emission appears to extend from the brighter peak toward the position of the fainter southeast one. The lower resolution B -, R -, and I -band images of Hu et al. (1993a) also showed similar structure and changes in morphology with wavelength. Morphological changes with wavelength are expected for bipolar reflection nebulae, as is illustrated in detail in the case of the Frosty Leo nebula (Langill, Kwok, & Hrivnak 1994).

The physical situation for IRAS 17150–3224 is clarified by examination of the emission profiles along the major axis of the nebula in each bandpass. These are displayed in Figure 3a. It is seen that as one progresses toward longer wavelength, an emission source between the two peaks increases in strength. This source appears to be somewhat closer to the weaker southeast peak. When allowance is made for this central emission peak of variable strength, we see that the two bipolar peaks remain at nearly the same positions and at about the same brightness ratios (3:1) in all three images. It is primarily the central source that is changing with wavelength. These color changes in the object can be viewed in two dimensions by examining a differential $V-I$ image, in the sense of the I image divided by the V image. We have first reduced the different sky levels to a similar value of ~ 100 counts, which in each case is about 1% of the peak emission value of the nebula. These images are then ratioed to obtain the I/V image shown in the upper

panel of Figure 4. Although the image is not properly flux calibrated, it does show the changes in color across the images. One can see a central bar of emission along the minor axis of the nebula, that is very red in color. This presumably represents light from a disk around the central star of this bipolar nebula. The disk is as red as the reddest star in the field, while the $V-I$ color of the lobes is as blue as any object in the field. The faint ringlike structures around the two lobes may be artifacts due to the larger seeing disk in the I image.

Both the V and I images of IRAS 17441–2411 display a bipolar nebula extended in the north-south direction. The angular size is estimated to be $10''.6 \times 7''.0$ in V and $11''.6 \times 7''.6$ in I . The average position angle is 17° for the inner core, as measured from the line connecting the two peaks, but it is somewhat less for the outer halo. No $H\alpha$ image of this object was obtained. The object is clearly an extended, bipolar nebula, with the two components have profiles that are significantly wider than point sources. It is not two close stars, as suggested by Hu et al. (1993b). The two peaks are separated by $1''.5$ in V and $1''.3$ in I . The relative brightnesses of the two peaks are similar in both colors, as can be seen by looking at the emission profiles along the major axis of the nebula. These are displayed in Figure 3b. Again, we can examine the color changes from the V to I band in two dimensions, and we did this in a similar manner as with IRAS 17150–3224. The differential $V-I$ image of IRAS 17441–2411 is shown in the bottom panel of Figure 4. In this case, there is not such a strong color-dependent component, although the peaks are somewhat closer together in the I band, and thus the nebula is redder in the center. A faint red bar appears in the $V-I$ image along the minor axis, again indicating the presence of a disk.

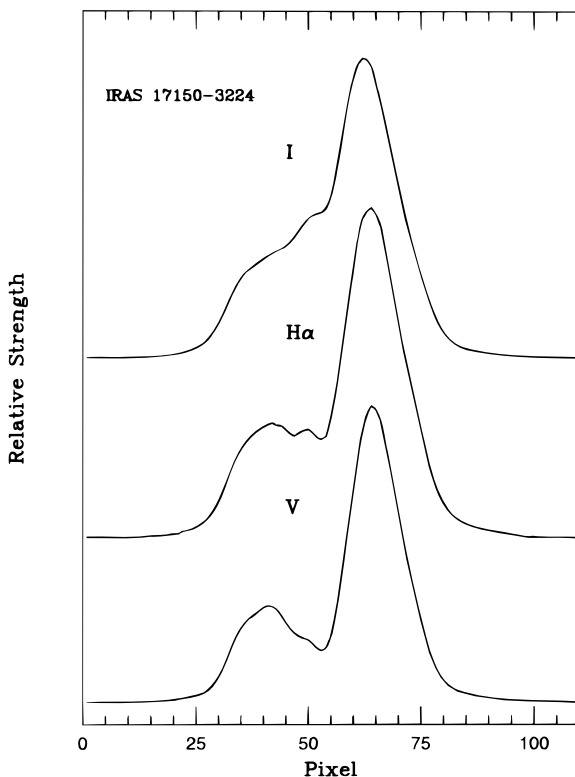


FIG. 3a

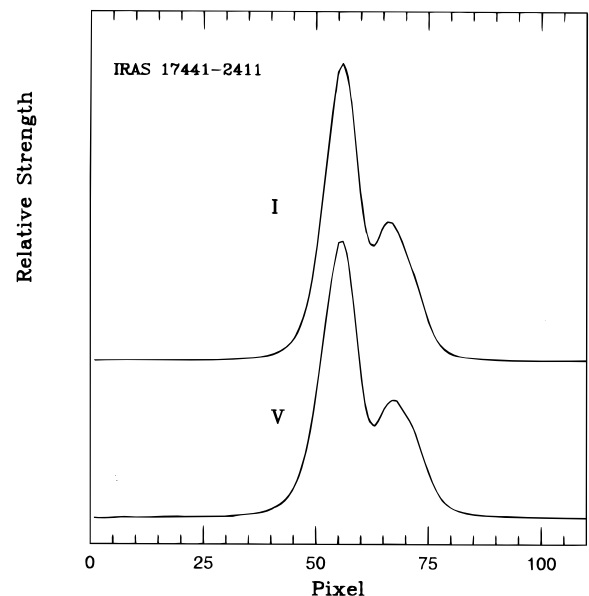


FIG. 3b

FIG. 3.—Emission profiles for (a) IRAS 17150–3224 and (b) IRAS 17441–2411 along the major axis in each bandpass

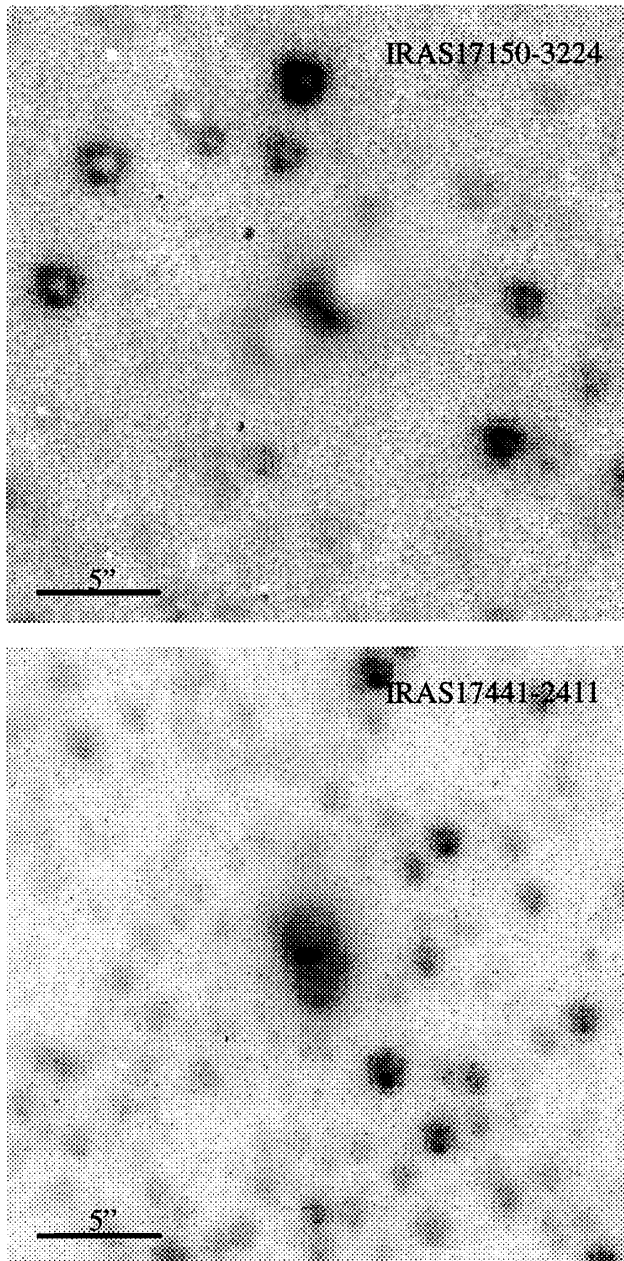


FIG. 4.—Gray-scale image of the differential $V-I$ color of IRAS 17150–3224 and IRAS 17441–2411. A red disk along the minor axis is seen clearly in each case. The darker the gray scale, the redder is the $V-I$ color.

Magnitude measurements were made for both of these objects, using aperture photometry in DAOPHOT. Since they are extended, a large aperture of $10''.4$ diameter was used, which included essentially all of the light of the nebulae. A number of photometric standard stars were observed, and these were reduced with a smaller aperture ($6''$). The V and I magnitude measurements were transformed to the standard Johnson and Cousins system, respectively, and they are listed in Table 2.

2.3. Near-Infrared Imaging

Near-infrared JHK images of IRAS 17150–3224 were obtained at the Cerro-Tololo Inter-American Observatory (CTIO) with the 1.5 m telescope in the infrared configu-

ration. The observations were made on 1992 May 10 under marginally photometric skies, using some time kindly made available by J. Wallin. A 62×58 element InSb array was used, which had a scale of $0''.89$ per pixel.

Images in all three bandpasses showed the object to be extended compared with field stars. The image sizes (FWHM) of the PPN in J , H , and K are $3''.3$, $2''.9$, and $2''.7$, respectively, compared with the field stars of $2''.3$. In all three images, the emission peak is in the center of the object. The object is clearly elongated in the J image, with a size of $11'' \times 7''.5$ and with a similar position angle to that seen in the visible. The H image appears slightly elongated, while in the K image this is not obvious. Note that Hu et al. (1993a) saw no extended emission in their K -band image (pixel size of $0''.9$); perhaps their resolution was significantly worse than ours.

2.4. Low-Resolution Mid-Infrared Spectra

Mid-infrared spectra of both objects have been obtained with the *IRAS* Low Resolution Spectrometer (LRS). Both show a very red continuum and a silicate absorption feature at $10 \mu\text{m}$; the feature is weaker in 17441–2411 but nevertheless present. These can be seen in Figures 5 and 6. The silicate feature must originate from very cold dust in order to appear in absorption against the cool (~ 180 K) dust continua. It is possible that the silicate feature, or at least some of it, is interstellar in origin, rather than circumstellar.

3. DISCUSSION

IRAS 17150–3224 was first suggested as a PPN candidate based on its infrared colors by van der Veen et al. (1989), and Volk & Kwok (1989). The object is identified with AFGL 6815S. From its optical spectrum, Hu et al. (1993a) suggested a spectral type of G2 I, consistent with the expectation of a post-AGB star. The SED of this object is shown in Figure 5. Although the “double-peak” nature of the object is clearly present, the photospheric component is much weaker than the dust component. This suggests that the central star is obscured by a circumstellar disk³ oriented perpendicular to the plane of the sky. The detection of the bipolar nebula in the plane of the sky (due to scattered light) and of the red disk seen along the minor axis are therefore consistent with the shape of the observed SED.

We have fitted the SED of IRAS 17150–3224 with two blackbody curves, indicating color temperatures of ~ 3000 and ~ 185 K for the reddened photosphere and the dust components, respectively. The amounts of flux received from the two components are $\sim 2.1 \times 10^{-10}$ and $\sim 5.7 \times 10^{-8} \text{ ergs s}^{-1} \text{ cm}^{-2}$, respectively. The total luminosity of the object as inferred from the observed flux is $1.9 \times 10^3 (D/\text{kpc})^2 L_{\odot}$. Assuming that it has the minimum luminosity of $\sim 3000 L_{\odot}$ required for a post-AGB star, then the observed flux suggests a minimum distance of 1.3 kpc. Since IRAS 17150–3221 lies in the direction of the galactic center ($l = 353^{\circ}8$, $b = 3^{\circ}0$), such a distance is not unreasonable. This distance yields a minimum diameter for the nebula of 0.10 pc.

The PPN nature of IRAS 17441–2411 was discussed first by Volk & Kwok (1989) and more recently by Hu et al.

³ Here we use the term “disk” to refer to the circumstellar region, which has a density gradient. In this sense, it is different from the meaning commonly used in other contexts, where it refers to a region of finite size and limited thickness.

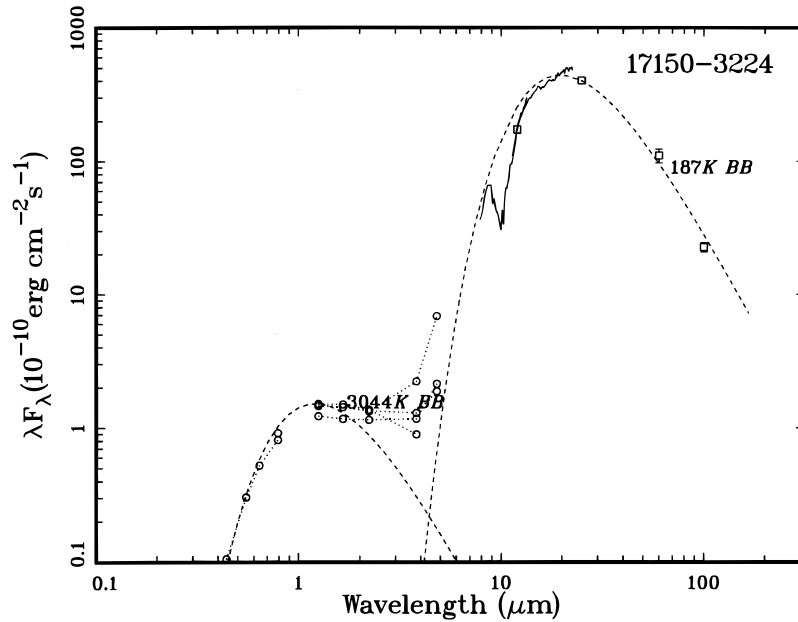


FIG. 5.—The spectral energy distribution of IRAS 17150–3224. Open circles between 0.5 and 5 μm are ground-based photometric observations from this paper and Hu et al. (1993a). Squares (with error bars) are color-corrected *IRAS* fluxes. the *IRAS* LRS spectrum is shown as a solid line between 8 and 23 μm and has been adjusted slightly to agree with the color-corrected *IRAS* 12 and 25 μm fluxes. Two blackbody curves (*dashed lines*) are fitted to the data to illustrate the color temperatures of the dust and photospheric continua. The blackbody temperatures are given next to the fittings.

(1993a). The SED of this object is plotted in Figure 6. The amounts of flux received from the photospheric and dust components are $\sim 2.3 \times 10^{-10}$ and $\sim 2.8 \times 10^{-8}$ ergs $\text{s}^{-1} \text{cm}^{-2}$, respectively. These fluxes correspond to a total luminosity of $\sim 8.5 \times 10^2 (D/\text{kpc})^2 L_{\odot}$. Assuming that it has the minimum luminosity of $\sim 3000 L_{\odot}$ for a post-AGB star, then the observed flux suggests a minimum distance of 1.9 kpc and a minimum diameter of the nebula of 0.11 pc. Since IRAS 17441–2411 also lies in the direction of the galactic center ($l = 4^{\circ}2$, $b = 2^{\circ}2$), such a distance is not unreasonable.

We have revealed for the first time, in the $V-I$ color images, the central circumstellar disks around two new

bipolar nebulae. The very red colors of the circumstellar disks are caused by severe extinction in the densest parts. The bluer colors of the lobes indicate the stellar light scattered by dust grains in the lobes. The optical images themselves trace primarily the distribution of scattered light, away from the denser parts (i.e., the disk) of the circumstellar envelope. In the subsequent evolution, after the nebulae are photoionized, the optical images will be dominated by recombination lines of H and He and collisionally excited lines of metals, whose strengths are proportional to the emission measure of the nebula. As the matter distribution also changes as the result of interacting winds, the optical morphologies are expected to change as the results of

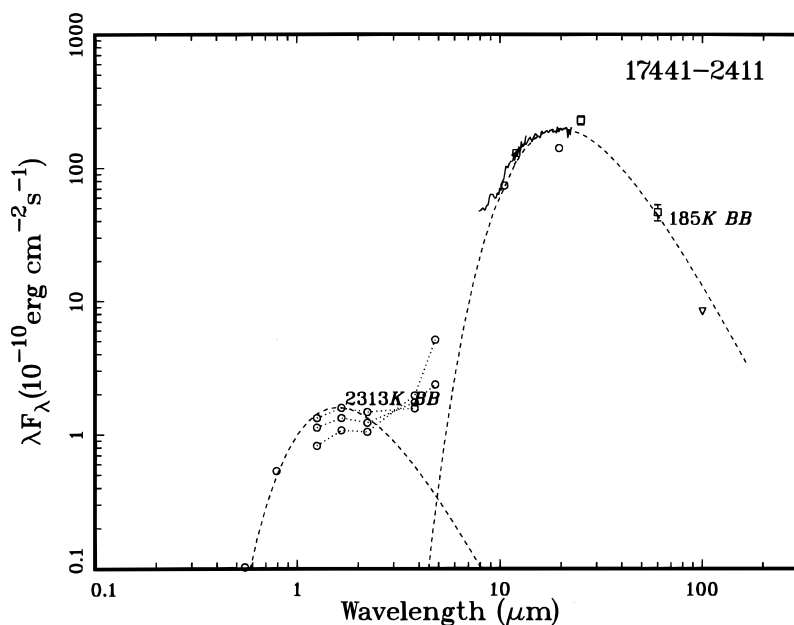


FIG. 6.—The SED of IRAS 17441–2411. Symbols are the same as in Fig. 5.

dynamics and photoionization. The important result of these images, however, is that the axisymmetry is already apparent in this early stage of post-AGB evolution.

4. CONCLUSION

High-resolution optical images have revealed the bipolar nature of two PPNs. The distribution of the scattered visible light seen in these images is consistent with the observed SED, which suggests that the central stars are each obscured by a circumstellar disk. These disks can be seen clearly in the $V-I$ images. The existence of these two bipolar objects, along with previously known bipolar PPNs such as AFGL 618 and AFGL 2688, suggests that bipolar morphology commonly occurs early in the evolution of PNs, even during the PPN phase before photoionization.

The density structures determined from these images will serve as important initial conditions for the hydrodynamical models.

We thank Kevin Volk for helpful discussions and Wenxian Lu for assistance with data reduction. The observing assistance at CFHT and UKIRT and the observations by Patricia Whitelock and John Wallin are much appreciated. This work is supported in part by a grant to S. K. from the Natural Sciences and Engineering Research Council, and in part by grants to B. J. H. from the NASA Astrophysics Data Program grant (NAG 5-1223) and the National Science Foundation (AST 90-18032, AST 93-15107).

REFERENCES

- Aaquist, O. B., & Kwok, S. 1996, *ApJ*, 462, 813
 Balick, B. 1987, *AJ*, 94, 671
 Balick, B., Rugers, M., Terzian, Y., & Chengalur, J. N. 1993, *ApJ*, 411, 778
 Curtis, H. D. 1918, *Publ. Lick Obs.*, XIII, 57
 Frank, A., & Mellema, G. 1994, *ApJ*, 430, 800
 Hrivnak, B. J., & Kwok, S. 1991, *ApJ*, 368, 564
 Hu, J. Y., Slijkhuis, S., de Jong, T., & Jiang, B. W. 1993b, *A&AS*, 100, 413
 Hu, J. Y., Slijkhuis, S., Nguyen-Q-Rieu, & de Jong, T. 1993a, *A&A*, 273, 185
 Kwok, S. 1982, *ApJ*, 258, 280
 ———. 1993, *ARA&A*, 31, 63
 Langill, P. P., Kwok, S., & Hrivnak, B. J. 1994, *PASP*, 106, 736
 Livio, M. 1995, in *Asymmetrical Planetary Nebulae*, ed. A. Harpaz & N. Soker (*Ann. Israel Phys. Soc.*, 11), 51
 McClure, R. D., et al. 1989, *PASP*, 101, 1156
 Mellema, G., & Frank, A. 1995, *MNRAS*, 273, 401
 Ney, E. P., Merrill, K. M., Becklin, E. E., Neugebauer, G., & Wynn-Williams, C. G. 1975, *ApJ*, 198, L129
 Pottasch, S. R. 1995, in *Asymmetrical Planetary Nebulae*, ed. A. Harpaz & N. Soker (*Ann. Israel Phys. Soc.*, 11), 7
 Price, S. D., & Murdock, T. L. 1983, *The Revised AFGL Infrared Catalog*, AFGL-TR-83-0161 (Washington: GPO)
 van der Veen, W. E. C. J., Habing, H. J., & Gaballe, T. R. 1989, *A&A*, 226, 106
 Volk, K. 1993, in *ASP Conf. Ser. Vol. 41, Astronomical Infrared Spectroscopy: Future Observational Directions*, ed. S. Kwok (San Francisco: ASP), 63
 Volk, K., & Kwok, S. 1989, *ApJ*, 342, 345
 Westbrook, W. E., Becklin, E. E., Merrill, K. M., Neugebauer, G., Schmidt, M., Willner, S. P., & Wynn-Williams, C. G. 1975, *ApJ*, 202, 407